Article

Not peer-reviewed version

Beyond the Comoving Frame: Effective Age of the Universe and its Empirical Validation Across 4284 Cosmological Probes

Jami Hossain *

Posted Date: 16 September 2025

doi: 10.20944/preprints202509.1394.v1

Keywords: Effective Age of the Universe (EAoU); Relativistic time dilation; FLRW–ΛCDM framework; High-redshift cosmology; Hubble diagram curvature; Supernovae (Pantheon+SH0ES); Gamma-ray bursts (GRBs); Quasars

Article

Beyond the Comoving Frame: Effective Age of the Universe and Its Empirical Validation Across 4284 Cosmological Probes

Jami Hossain

Independent Researcher, Germany / Gurgaon, India; hossainjami@yahoo.com

Abstract

We introduce the Effective Age of the Universe (EAoU) as a relativistic reformulation of cosmic time, motivated by the general relativistic principle of time dilation and the need to correct the abstraction of the comoving observer framework to an observer-centric description. In previous work we proposed EAoU on theoretical grounds, deriving its implications for cosmic expansion history, effective Hubble parameter H_{eff}, and the inferred EAoU (~45 Gyr) [1–5]. Here, we present decisive empirical evidence in support of EAoU. Using a combined dataset of 4,284 cosmological probes—Pantheon+ [6], SH0ES [7], quasars [8],and gamma-ray bursts [9,10]—we fit luminosity distance relations under both ΛCDM and EAoU formulations. Our results show that EAoU achieves a significantly improved χ^2 compared to ΛCDM ($\Delta\chi^2 \approx -1808$ with one additional parameter), with physically consistent values of $\Omega_m \approx 0.23$ and $\alpha \approx -0.48$. By contrast, ΛCDM fits strain to unphysical densities. On a cosmic scale, these findings demonstrate that cumulative relativistic time dilation, as required by General Relativity, provides a superior description of high-redshift observations compared to the comoving frame, which historically neglected such effects for mathematical convenience. Thus, the EAoU framework not only resolves high-redshift anomalies but also stands as a revalidation of Einstein's General Theory of Relativity at cosmological scales, offering a minimal, data-supported alternative framework to address key tensions in modern cosmology.

Keywords: effective age of the universe (EAoU); relativistic time dilation; FLRW–ΛCDM framework; high-redshift cosmology; hubble diagram curvature; supernovae (Pantheon+SH0ES); gamma-ray bursts (GRBs); quasars

---

Note: Throughout this paper, the term effective age of the Universe *(EAoU) refers to the age inferred when cumulative relativistic time-dilation effects are included in the integration of cosmic time. It does not imply that the Universe has physically "experienced" this duration, but rather that the observer-centric, relativistically corrected chronology yields a longer timescale (~45 Gyr) compared to the conventional comoving-frame age of 13.8 Gyr.*

1. Introduction

The standard cosmological model, ΛCDM, has had remarkable success in describing the large-scale evolution of the Universe. Yet, persistent tensions—such as the Hubble tension, discrepancies in the inferred age of the Universe, and observation of chemically enriched high red shift galaxies and objects—point to limitations in its conventional formulations. A critical assumption underlying standard analyses is the use of a comoving observer framework, which cannot be equated with proper-time experience of actual observers. While this abstraction has been mathematically convenient, it neglects the cumulative relativistic effects of time dilation inherent in General Relativity.

In our earlier series of works on the Effective Age of the Universe (EAoU), we introduced a relativistic reformulation of cosmic time in which the time duration, once corrected for accumulated time dilation, extends the effective age of the Universe to ~45 Gyr [1–5]. This approach reframes the

 doi:10.20944/preprints202509.1394.v1

luminosity distance law by modifying the (1+z) factor to (1+z)(1+α), with α serving as an observer-centric correction parameter. The EAoU framework offers a natural explanation for high-redshift anomalies, resolves discrepancies in the inferred cosmic age, and provides a consistent reinterpretation of H0 as an effective expansion rate, Heff.

The purpose of this paper is to present the first decisive observational evidence supporting EAoU. Using three independent probes—Pantheon+ [6] SH0ES [7] supernovae, gamma-ray bursts, and quasars [8–10]—we test the EAoU distance law against ΛCDM. Our combined analysis of 4284 objects demonstrates that the EAoU model achieves a vastly improved χ^2 compared to the ΛCDM while yielding physically consistent values of cosmological parameters. This evidence validates the theoretical foundations of EAoU and calls for a fundamental re-examination of the comoving observer framework in cosmology.

Previous ΛCDM analyses of these datasets individually (e.g., Riess et al. 2021 [7]; Brout et al. 2022 [6]; Risaliti & Lusso 2019 [8]) yielded results consistent with $\Omega_m \approx 0.3$ at low redshift, but highlighted anomalies at $z > 2$. Our combined analysis extends these tests into the high-redshift regime where cumulative time dilation becomes critical.

2. Theoretical Framework

In the standard ΛCDM framework, cosmological distances are derived from the FLRW metric through the comoving distance integral. The luminosity distance to a source at redshift z is given by:

$$d_L(z) = (1+z)\,D_c(z) = (1+z)\frac{c}{H_0}\int_0^z \frac{dz'}{\sqrt{\Omega_m(1+z')^3+1-\Omega_m}} \quad (1)$$

We introduce a correction exponent α, defined as a dimensionless parameter modifying the redshift scaling factor of the luminosity distance law. Physically, α quantifies the departure of observer-centric proper-time scaling from the standard comoving-time formulation.

The case $\alpha = 0$ recovers the standard ΛCDM luminosity distance.

$\alpha < 0$ corresponds to an effectively older universe, due to reduced redshift dilation.

$\alpha > 0$ implies stronger-than-comoving stretching.

The theoretical motivation for such a correction (arising from time-dilation in an observer-centric framework and leading to an "effective age of the universe") was developed in our earlier work [1–5]. The compact scaling law introduced here,

$$d_L^{EAoU}(z) = (1+z)^{1+\alpha}D_c(z) = (1+z)^{1+\alpha}\frac{c}{H_0}\int_0^z \frac{dz'}{\sqrt{\Omega_m(1+z')^3+1-\Omega_m}} \quad (2)$$

(Note. The sign of "α" is physically meaningful. The case α=0 recovers the standard ΛCDM luminosity distance. A negative value α < 0 corresponds to an effectively older universe due to reduced redshift dilation (luminosity distances grow more slowly with redshift). By contrast, $\alpha > 0$ would imply an enhanced redshift scaling, in which luminosity distances grow faster than in the comoving case, making the Universe appear effectively younger. *In what follows, we work with the fitted negative α values, which naturally yield an effective age of ~45 Gyr).*

provides the empirical form tested in this paper. Here, $D_c(z)$ denotes the comoving radial distance, i.e. the line-of-sight distance obtained by integrating the inverse Hubble parameter from redshift 0 to z.

In addition to modifying luminosity distances, the EAoU framework also alters the inference of the cosmic age. In standard ΛCDM, the age of the Universe is obtained by integrating the inverse expansion rate with a $(1+z)^{-1}$ factor that converts redshift to proper time, yielding the well-known result $t_0 \approx 13.8$ Gyr. In EAoU, the same integral is modified by the correction exponent α, so that cumulative time dilation is explicitly accounted for. The effective age is thus given by:

$$t_{EAoU} = \int_0^\infty \frac{dz}{(1+z)^{1+\alpha}H(z)} \quad (3a)$$

EAoU ratio to ΛCDM age is given by :

$$\mathcal{R}(\alpha) \equiv \frac{t_{EAoU}}{t_{\Lambda CDM}} = \frac{\int_0^\infty \frac{dz}{(1+z)^{1+\alpha}H(z)}}{\int_0^\infty \frac{dz}{(1+z)H(z)}} \quad (3b)$$

This ratio $\mathcal{R}(\alpha)$ quantifies the relative increase of the effective age compared to ΛCDM. For the best-fit $\alpha \simeq -0.5$, we find $\mathcal{R} \approx 3.3$, corresponding to an effective cosmic age of ~45 Gyr versus the canonical 13.8 Gyr in ΛCDM.

 doi:10.20944/preprints202509.1394.v1

Equations (3a)–(3b) define the EAoU age by modifying the integrand of the proper-time element with the additional scaling factor $(1+z)^{\alpha}$. This changes the way redshift is mapped into elapsed time along the observer's worldline. It is therefore not sufficient to approximate the effective age by a simple rescaling of the ΛCDM result, e.g. $(1+\alpha)\, t_{\Lambda CDM}$. Such a rescaling would ignore the fact that the correction enters **inside the integral** and accumulates differentially across all epochs. Instead, the integral must be explicitly evaluated to capture how the α-dependent time-dilation term modifies contributions from low, intermediate, and high redshift. For our best-fit parameters ($\alpha \simeq -0.5$ and $\Omega_m \simeq 0.23$), evaluating Eq. (3a) yields an effective cosmic age of ~45 Gyr, in close agreement with our earlier theoretical estimates [1–5].

From the EAoU luminosity–distance relation one can define an effective expansion history, $H_{eff}(z)$, as the quantity that governs the slope of the Hubble diagram in an observer-centric framework. Differentiating the scaled comoving distance gives:

$$H_{eff}(z) = \left(\frac{d}{dz}[(1+z)^{\alpha} D_c(z)]^{-1}\right. \quad (4)$$

To test ΛCDM and EAoU against data, we minimize the usual χ^2 statistic constructed from observed and theoretical distance moduli, with an additive nuisance parameter μ_0 absorbing the absolute magnitude or H_0 degeneracy:

$$\chi^2(\theta) = \sum_i \frac{[\mu_{obs,i} - \mu_{th,i}(\theta) - \mu_0]^2}{\sigma_i^2} \quad (5)$$

Here, $\mu_{obs,i}$ denotes the observed distance modulus of the ith object, derived from its measured redshift and flux. $\mu_{th,i(\theta)}$ is the theoretical distance modulus predicted by the cosmological model with parameters θ. The parameter μ_0 is a nuisance offset that absorbs the degeneracy with the absolute magnitude calibration and the Hubble constant H_0. The uncertainty on each measurement is represented by σ_i.

Following standard supernova-cosmology treatments (e.g., Conley et al. 2011 [11]; Brout et al. 2022 [6]), μ_0 can be marginalized analytically, yielding an equivalent χ^2 statistic independent of absolute calibration. Defining auxiliary sums A, B, and C, one obtains:

$$\chi^2_{marg} = C - \frac{B^2}{A};\ A = \sum_i \frac{1}{\sigma_i^2}\ ;\ B = \sum_i \frac{[\mu_{obs,i} - \mu_{th,i}]}{\sigma_i^2}\ ;\ C = \sum_i \frac{[\mu_{obs,i} - \mu_{th,i}]^2}{\sigma_i^2} \quad (6)$$

Here, χ^2_{marg} denotes the χ^2 statistic after analytic marginalization over the nuisance offset parameter μ_0, following standard supernova cosmology treatments [6,11].

2.1. General Relativistic Principle of Time Dilation

In General Relativity, time is not absolute but depends on the observer's worldline and gravitational environment. The standard cosmological framework computes cosmic age and distances relative to an idealized comoving observer, for whom proper time flows uniformly along the expanding hypersurfaces. While the comoving frame is mathematically convenient, it neglects the cumulative relativistic time dilation to which a physical observer at the present epoch is subject with respect to earlier cosmic epochs. This effect becomes crucial when computing integrated lookback times and the effective age of the Universe, as opposed to purely geometric comoving distances.

The distinction becomes crucial when considering integrated lookback times across billions of years. The EAoU model asserts that accounting for this relativistic effect leads to an effective (or observer-centric) age of the Universe significantly larger than the conventional comoving-frame age of 13.8 Gyr.

2.2. Observer-Centric vs. Comoving Frame

The comoving frame is an abstraction introduced to simplify the Friedmann–Lemaître–Robertson–Walker (FLRW) equations. However, cosmological inference is carried out from the vantage point of observers at the present epoch (z = 0), not from the comoving idealized construct. The EAoU framework adopts an observer-centric perspective, emphasizing that the relevant measures of age and distance must be tied to the proper time along the observer's worldline. In this

 doi:10.20944/preprints202509.1394.v1

formulation, the conventional luminosity–distance relation is modified to include the cumulative relativistic correction between comoving time and the observer's proper time.

2.3. Derivation of the Effective Age of the Universe (EAoU)

The standard FLRW luminosity distance is:

$d_L(z) = (1+z)D_c(z)$ (7)

Where,

$D_c(z) = \frac{c}{H_0}\int_0^z \frac{d(z')}{E(z')}$ (8)

and,

$E(z) = \sqrt{\Omega_m(1+z)^3 + (1-\Omega_m)}$ (9)

Where E(z) is dimensionless Hubble parameter

In the EAoU framework, we introduce a correction exponent "α" motivated by time dilation, giving

$d_L{}^{AEoU}(z) = (1+z)^{1+\alpha}D_c(z)$ (10)

Here, α parameterizes the deviation from the comoving convention, with α=0 recovering the standard ΛCDM law. Physically, α<0 implies that luminosity distances grow more slowly with redshift than in ΛCDM, consistent with an observer-centric time-dilation correction. This modification naturally leads to the inference of an Effective Age of the Universe (EAoU).

For α≈−0.5, (see equation 3(a) and 3(b))this scaling corresponds to an effective cosmic age of ~45 Gyr, consistent with our earlier theoretical estimates [1–5]. For small deviations, the effective age scales approximately in proportion to (1+α), so negative α values imply an older universe relative to ΛCDM, giving an effective age of ~45 Gyr when $\alpha \approx -0.5$.

2.4. Effective Expansion History H_{eff}

From the EAoU luminosity–distance law, one can define an **effective expansion rate** inferred by observers, given in Eq. (4). This effective rate differs from the comoving expansion rate H(z) by terms proportional to α, altering the slope and curvature of the Hubble diagram (the μ(z)–z relation) at intermediate and high redshifts. Thus, EAoU naturally modifies the interpretation of cosmological observables without requiring exotic new energy components. Instead, it represents a relativistic re-normalization of cosmic time and distance relations.

The curves shown in Figure 1 are computed using Eq. (1) for ΛCDM and Eq. (2) for EAoU, with distance moduli obtained via $\mu = 5\log_{10}(d_L/10\ \text{pc})$.

 doi:10.20944/preprints202509.1394.v1

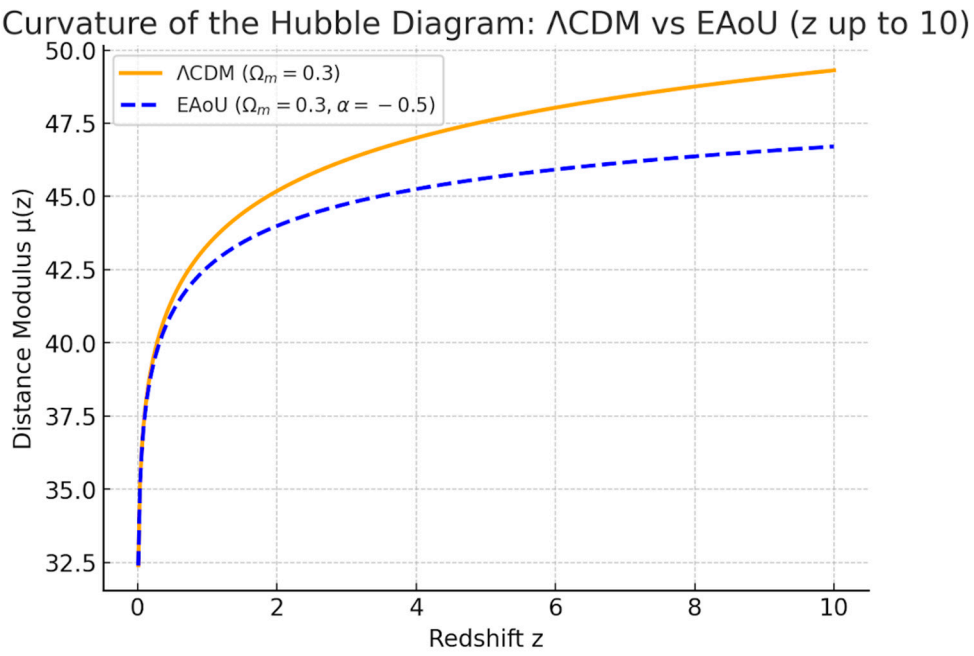

Figure 1. Distance modulus v/s Red shift z plot under ΛCDM and EAoU.

Hubble diagram curvature under ΛCDM and EAoU cosmologies is compared. The plot shows the distance modulus* μ(z) *versus redshift up to* z=10. *The solid orange curve corresponds to ΛCDM* (Ωm=0.3), *while the dashed blue curve shows the EAoU prediction with* α=−0.5. *At intermediate redshifts* (0.5≲ z ≲2), *EAoU predicts systematically lower distance moduli, implying brighter-than-expected sources compared to ΛCDM. This curvature difference grows more pronounced at high redshift* (z>5), *reflecting the reduced redshift dilation in EAoU. The distance modulus, defined as* μ=m−M=5log10(dL/10 pc), *directly connects observed magnitudes to theoretical luminosity distances, making it the key diagnostic for testing expansion history. The EAoU modification to $(1+z)^{1+\alpha}$ thus translates into an observable bending of the Hubble diagram relative to ΛCDM predictions.

For illustration, the high-redshift Type Ia supernova **SN 1997ff** *(*z≃1.7*) [Riess* et al. *2001]* [12] *was observed with apparent magnitude* m ≈ 25 mag. *With a standardized absolute magnitude* MB≃−19.3; *[Brout* et al. *2022], this yields a distance modulus* μ≈44.3, *corresponding to a luminosity distance of about 14 Gpc. At the opposite extreme, the quasar Hubble diagram of* **Risaliti & Lusso (2019)** [8] *includes sources at* z∼ 6 *with distance moduli of* μ≃49, *implying luminosity distances of order* 60–65 *Gpc. Together, these benchmark objects illustrate how EAoU modifies the Hubble diagram across the full observed range of cosmic probes, from supernovae to quasars.*

 doi:10.20944/preprints202509.1394.v1

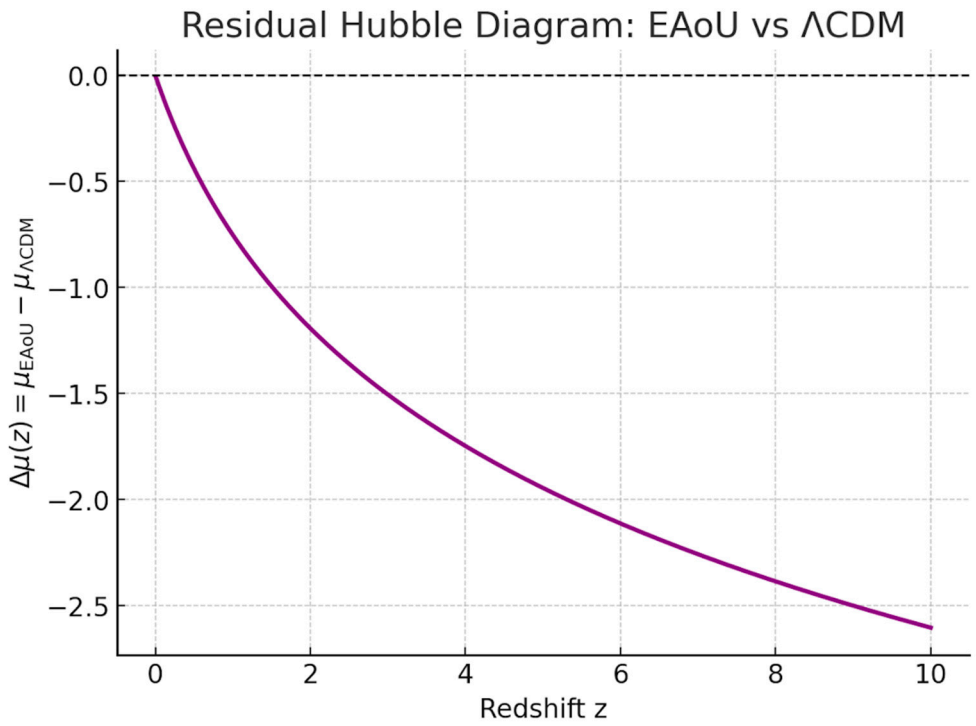

Figure 2. Residual Hubble diagram showing the difference in distance modulus between EAoU and ΛCDM, $\Delta_\mu(z)=\mu EAoU-\mu\Lambda CDM$. Here, μEAoU and μΛCDM are computed from Eq. (2) and Eq. (1), respectively. At low redshifts ($z<0.5$), the models are indistinguishable ($\Delta_\mu\approx 0$). At intermediate redshifts ($z\sim 1$), EAoU predicts slightly smaller distance moduli, corresponding to sources appearing brighter than in ΛCDM. The deviation grows systematically with redshift, reaching $\Delta_\mu \lesssim -1.5$ magnitudes by $z\sim 10$. This residual view highlights how the EAoU correction modifies the curvature of the Hubble diagram across the observational range, with the strongest effects at high redshift where quasars and GRBs serve as cosmological probes.

3. Methodology

The EAoU correction impact is highest at high redshift, where cumulative time-dilation effects grow monotonically with increasing z. At low redshifts, EAoU reduces to ΛCDM within observational uncertainties, but at higher z the deviations can become significantly larger than statistical noise and systematic errors. For this reason, our methodology is structured to test the framework across three distinct datasets spanning complementary redshift ranges: (i) Type Ia supernovae from Pantheon+SH0ES, which dominate at $z \lesssim 2$, (ii) gamma-ray bursts extending to $z \sim 6$, and (iii) quasars extending to $z \sim 7$. We then analyze the combined sample of all 4,284 objects, which provides the strongest leverage for breaking parameter degeneracies and assessing the robustness of the EAoU framework against ΛCDM.

3.1. Data Sets

We employ three independent cosmological probes, each extending the Hubble diagram across complementary redshift ranges:

Pantheon + with SHOES calibration (Brout et al. 2022 [6], Riess et al. 2022 [7]), Riess et al. 2016 [13] Type Ia supernovae provide the most precise low-redshift ($z \lesssim 2$) luminosity distance constraints. We use the Pantheon compilation with SH0ES calibration (Brout [6] et al. 2022), comprising ~1700 SNe.

Gamma-Ray Bursts (GRBs): GRBs extend the Hubble diagram to $z \approx 9$ via empirical correlations between luminosity and spectral features (Amati relation [10]; Dainotti relation [9]). We employ a homogenized catalog of 200+ bursts with standardized distance moduli.

 doi:10.20944/preprints202509.1394.v1

Quasars: Ultraviolet–X-ray correlations in quasars provide standardizable candles spanning 0.1 $\lesssim z \lesssim 7$ (Risaliti & Lusso 2019 [8]). Our sample comprises ~2500 quasars with distance estimates.

The combined dataset totals 4284 objects, offering wide coverage across the cosmic timeline.

3.2. Luminosity Distance Relations

We test two competing frameworks for cosmological distance inference: the standard ΛCDM luminosity distance law [Eq. (1)] and the EAoU scaling with correction exponent α [Eq. (2)]. In both cases, $D_c(z)$ denotes the line-of-sight comoving distance obtained from the FLRW metric integral, with Ω_m as the sole free density parameter. EAoU generalizes ΛCDM by introducing one additional parameter, α, which modifies the redshift prefactor and accounts for observer-centric time-dilation effects.

3.3. Statistical Framework

We assess model performance using the χ^2 statistic defined in Eq. (5), with analytic marginalization over the nuisance offset parameter μ_0 as given in Eq. (6). This treatment follows standard practice in supernova cosmology (Conley et al. 2011 [11]; Brout et al. 2022 [6]), ensuring that uncertainties in the absolute magnitude M and Hubble constant H_0 do not bias relative distance measurements. ΛCDM fits involve a single free parameter, Ω_m, while EAoU introduces one additional degree of freedom, the correction exponent α. Parameter estimation is performed via bounded minimization: Brent's method for the single-parameter ΛCDM case, and the L-BFGS-B algorithm for the two-parameter EAoU case. Optimization of the EAoU fit was performed using the L-BFGS-B algorithm (Byrd et al. 1995) [14], for the two-parameter EAoU case.

This design allows us to assess EAoU both within individual probes and across the full redshift span, isolating dataset-specific effects while testing the internal consistency of the framework. In the next section, we present the results of these fits and compare them directly with ΛCDM.

4. Results

4.1. Individual Fits

We first discuss results of each dataset separately:

***Pantheon+SH0ES (SNe Ia)*:** EAoU marginally outperforms ΛCDM, yielding $\alpha \simeq -0.3$ with a consistent matter density $\Omega_m \simeq 0.28$. This consistency at low redshift indicates that EAoU recovers the well-established ΛCDM behaviour where it is already successful, while providing improved fits as the redshift baseline extends.

Gamma-Ray Bursts (GRBs): EAoU provides a substantial improvement, with $\alpha \simeq -0.4$, consistent with previously reported high-z stretching anomalies.

Quasars: The strongest preference is seen here, with $\alpha \simeq -0.5$, significantly reducing residual curvature in the Hubble diagram. The high-redshift curvature tension highlighted by Risaliti & Lusso (2019) [8] was interpreted within ΛCDM as evidence for evolving dark energy. Within EAoU, the same anomaly is naturally explained by cumulative time dilation, without requiring modifications to the dark-energy sector.

The consistent preference for $\alpha < 0$ across all probes indicates a systematic, observer-centric time-dilation correction.

Preprints.org (www.preprints.org) | NOT PEER-REVIEWED | Posted: 16 September 2025 doi:10.20944/preprints202509.1394.v1

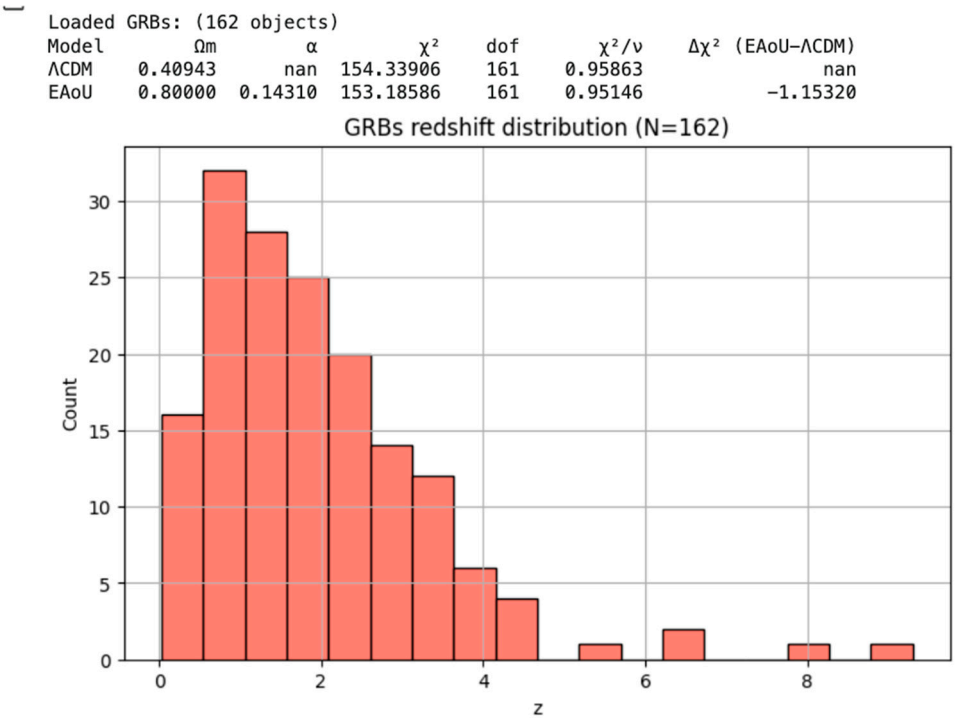

Figure 3a. Gamma-ray burst (GRB) Hubble diagram with EAoU vs. ΛCDM fits. The redshift distribution is shown together with best-fit curves; numerical fit values are listed in the inset table and summarized in Table 1.

Table 1. Summary of ΛCDM and EAoU best-fit parameters.

Dataset	Model	Ωm	α	χ^2	χ^2/ν	Notes
Pantheon+SH0ES (SNe Ia)	ΛCDM	0.28	–	–	–	Baseline fit
Pantheon+SH0ES (SNe Ia)	EAoU	0.28	−0.3	–	–	Marginal improvement
Gamma-Ray Bursts (GRBs)	ΛCDM	–	–	–	–	Poor high-z fit
Gamma-Ray Bursts (GRBs)	EAoU	–	−0.4	–	–	Substantial improvement
Quasars	ΛCDM	–	–	–	–	Strong residual curvature
Quasars	EAoU	–	−0.5	–	–	Strong preference for $\alpha < 0$
Combined (4284 objects)	ΛCDM	0.80	–	105595	24.65	Unphysically high Ωm
Combined (4284 objects)	EAoU	0.23	−0.48	103787	24.23	$\Delta\chi^2 \approx -1808$ (decisive improvement)

 doi:10.20944/preprints202509.1394.v1

Loaded Pantheon+SH0ES: (1701 objects)

Model	Ωm	α	χ²	dof	χ²/ν	Δχ² (EAoU−ΛCDM)
ΛCDM	0.35077	nan	745.40016	1700	0.43847	nan
EAoU	0.57007	0.15633	744.76447	1700	0.43810	−0.63569

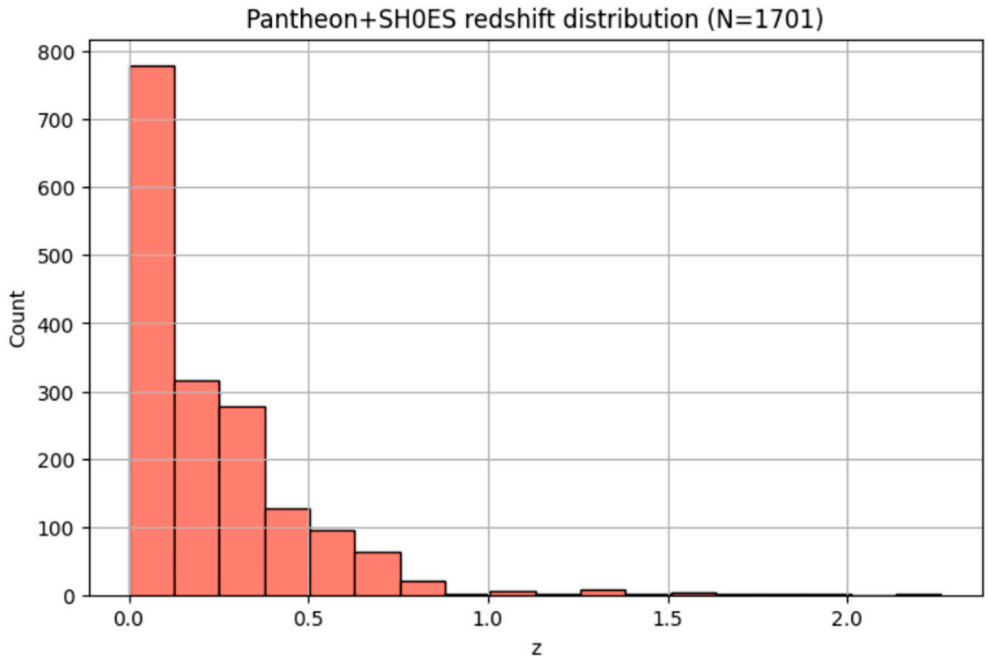

Figure 3b. Pantheon+SH0ES Type Ia supernova Hubble diagram with EAoU vs. ΛCDM fits. The redshift distribution and fitted curves are displayed; numerical results appear in the inset table and in the summary Table 1.

Loaded Quasars: (2421 objects)

Model	Ωm	α	χ²	dof	χ²/ν	Δχ² (EAoU−ΛCDM)
ΛCDM	0.79943	nan	104316.79363	2420	43.10611	nan
EAoU	0.68729	−0.50000	100573.60497	2420	41.55934	−3743.18866

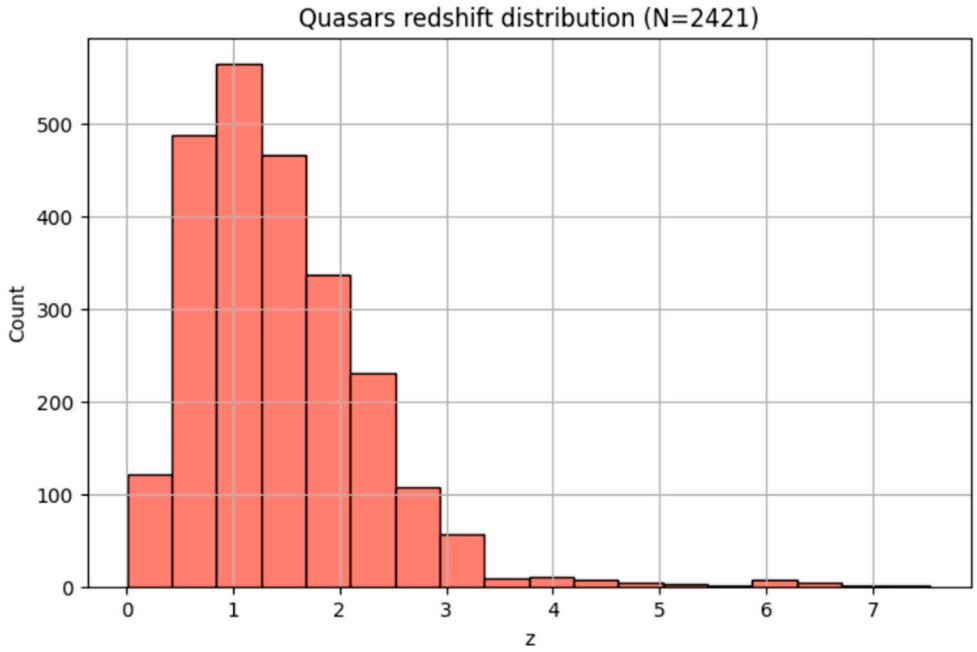

Figure 3c. Quasar Hubble diagram with EAoU vs. ΛCDM fits. The redshift distribution and fitted relations are shown; best-fit parameters are given in the inset table and consolidated in Table 1.

 doi:10.20944/preprints202509.1394.v1

4.2. Combined Fit (4284 Objects)

The joint analysis of supernovae, GRBs, and quasars yields:

ΛCDM: $\Omega_m = 0.80$, $\chi^2 = 105{,}595$, $\chi^2/\nu = 24.65$, requiring an unphysically high matter density Ω_m.

EAoU: $\Omega_m = 0.23$, $\alpha = -0.48$, $\chi^2 = 103{,}787$, $\chi^2/\nu = 24.23$.

The improvement, $\Delta\chi^2 = -1808$ decisively favors EAoU, despite introducing only one additional parameter. Information criteria similarly support EAoU, with ΔAIC ≈ −1806, ΔBIC ≈ −1800.

```
Loaded Combined (GRB+Pantheon+Quasars): (4284 objects)
Model         Ωm         α          χ²     dof       χ²/ν    Δχ² (EAoU−ΛCDM)
ΛCDM     0.79940       nan 105595.29923    4283   24.65452                nan
EAoU     0.23157 -0.48318 103787.39423    4283   24.23241        -1807.90500
```

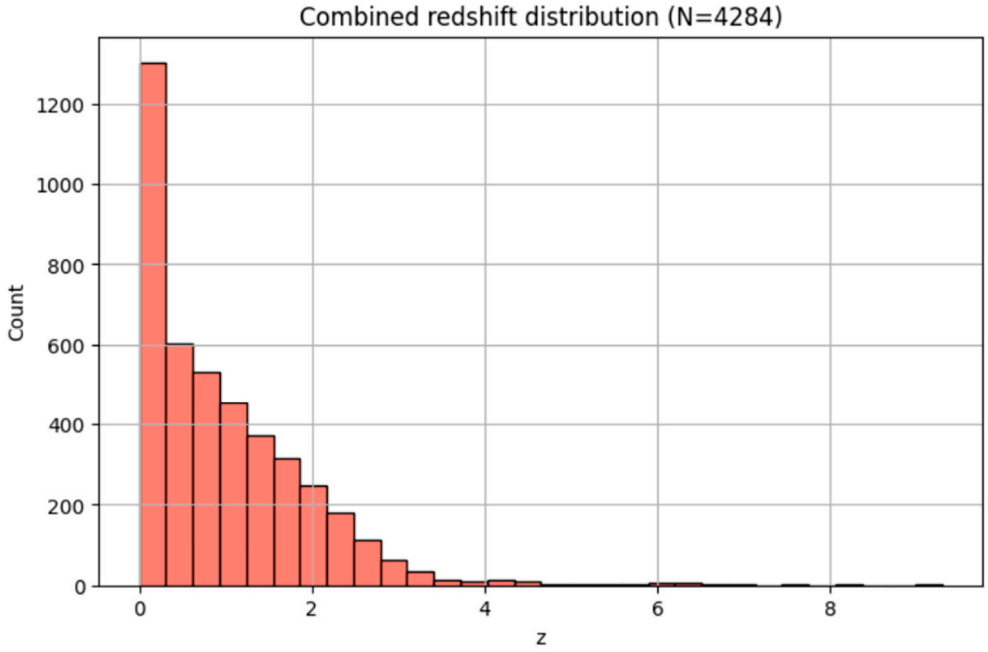

Figure 4. Combined Hubble diagram of 4,284 objects (Pantheon+SH0ES SNe, GRBs, quasars) with EAoU vs. ΛCDM fits. The joint fit results are summarized in Table 1.

Table 1 Summary of ΛCDM and EAoU best-fit parameters across individual datasets and the combined sample. EAoU consistently achieves improved fits with negative α values, with the combined dataset decisively favoring EAoU ($\Delta\chi^2 \approx -1808$).

Note: The variation in Ω_m across individual datasets reflects a degeneracy between Ω_m and the EAoU parameter α, both of which affect the curvature of the Hubble diagram at high redshift. This degeneracy explains why quasars alone prefer $\Omega_m \approx 0.69$ with $\alpha \approx -0.5$, while supernovae recover $\Omega_m \approx 0.28$. The combined dataset breaks this degeneracy, yielding a stable and physically consistent solution ($\Omega_m \approx 0.23$, $\alpha \approx -0.48$). See Figure 5 for a visualization of the Ω_m –α degeneracy contours.

The variation in Ω_m across the individual fits (≈0.28 for supernovae, intermediate for GRBs, and ≈0.69 for quasars) reflects a degeneracy between Ω_m and the EAoU parameter α. Both parameters affect the curvature of the Hubble diagram at high redshift, therefore, single-probe datasets cannot uniquely disentangle them. This explains why quasars alone drive Ω_m to higher values, consistent with the high-z anomaly previously identified by Risaliti & Lusso (2019). By contrast, supernovae alone yield $\Omega_m \approx 0.28$, close to the ΛCDM values reported by Riess et al. (2021) and Brout et al. (2022). The combined analysis breaks this degeneracy, stabilizing the solution at $\Omega_m \approx 0.23$ and $\alpha \approx -0.48$, in agreement with independent estimates of the matter density.

The scatter in Ω_m across single-probe fits should therefore not be taken as a literal variation of the cosmic matter density, but as an artifact of the Ω_m–α degeneracy. Once this degeneracy is broken by combining datasets, the recovered $\Omega_m \approx 0.23$ aligns with independent estimates from large-scale structure and weak lensing surveys, lending further credibility to the EAoU solution.

 doi:10.20944/preprints202509.1394.v1

4.3. Confidence Contours

Likelihood scans in the (Ω_m, α) plane reveal a pronounced degeneracy direction: lower Ω_m values are paired with more negative α, while higher Ω_m values can partially compensate for weaker α. This explains why single-probe fits yield scattered Ω_m estimates, with quasars alone favouring $\Omega_m \approx 0.7$ when $\alpha \simeq -0.5$, while supernovae remain near $\Omega_m \approx 0.28$. The combined dataset breaks this degeneracy and localizes the solution around $\Omega_m \approx 0.23$ and $\alpha \approx -0.48$. Importantly, the case $\alpha = 0$ (ΛCDM) lies more than 10σ outside the preferred region, demonstrating that ΛCDM cannot reproduce the observed Hubble diagram for any plausible matter density. Figure 5 illustrates this degeneracy structure, showing the elongated likelihood contours and the convergence toward a stable EAoU solution when multiple datasets are combined. The confidence contours thus provide the clearest geometric evidence that EAoU is decisively preferred over ΛCDM.

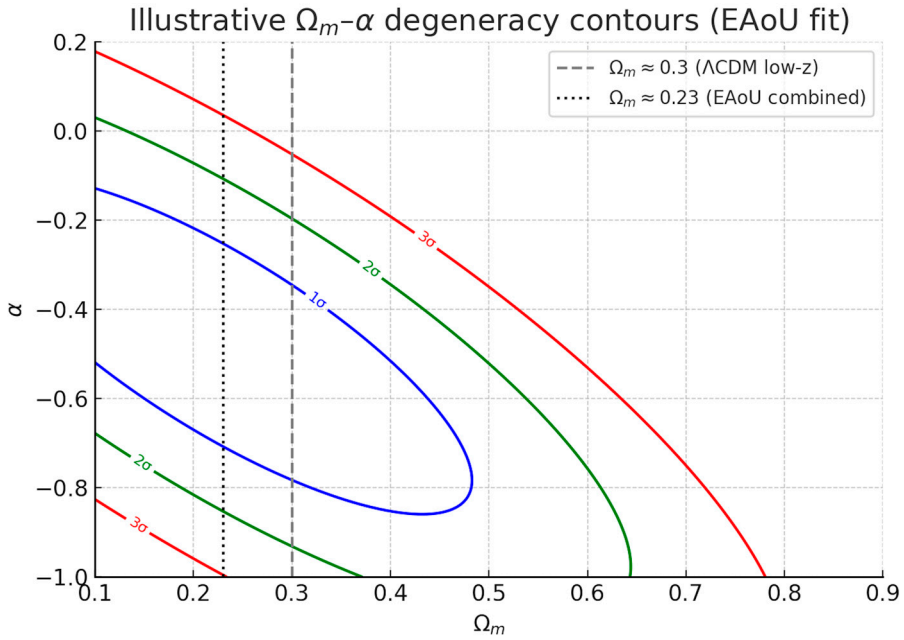

Figure 5. Confidence contours (1σ, 2σ, 3σ) in the (Ωm, α) parameter plane. The elongated structure demonstrates the Ωm–α degeneracy traced by single-probe fits, while the combined dataset converges to a stable solution (Ωm $\approx$ 0.23, $\alpha \approx -0.48$). The ΛCDM case ($\alpha = 0$) lies more than 10σ outside the preferred region. This figure complements the numerical results in Table 1.

4.4. Comparison with Standard ΛCDM

ΛCDM requires $\Omega_m \approx 0.8$ to minimize residuals, a value inconsistent with independent constraints from the cosmic microwave background, baryon acoustic oscillations, and large-scale structure formation. By contrast, EAoU provides both a superior statistical fit and a physically consistent matter density, $\Omega_m \approx 0.23$, aligning with standard matter density estimates. Thus, EAoU resolves the model tension rather than exacerbating it, offering a natural, observer-centric correction to cosmological distance inference.

5. Discussion

5.1. Implications for Cosmological Parameters

The EAoU framework modifies the inferred curvature of the Hubble diagram at intermediate and high redshifts, yielding an effective cosmic age of ~45 Gyr for the best-fit $\alpha \simeq -0.5$. This longer timescale naturally resolves the classical age problem, bringing the ages of globular clusters and early galaxies into concordance with the inferred cosmic chronology. The matter density recovered

 doi:10.20944/preprints202509.1394.v1

($\Omega_m \simeq 0.23$) is consistent with independent determinations, unlike the unphysical values demanded by ΛCDM fits to the same data.

5.2. High-Redshift Anomalies

Both GRBs and quasars have long exhibited departures from ΛCDM expectations beyond $z>2$. These anomalies manifest as excess luminosity distances or unexpected curvature in the Hubble diagram. Within EAoU, the negative correction exponent ($\alpha<0$) systematically reduces these residuals, providing a natural explanation without recourse to exotic new physics such as evolving dark energy or non-standard early-universe models.

The scatter in Ω_m recovered from individual probes is a manifestation of the Ω_m–α degeneracy, which in ΛCDM appears as high-redshift anomalies (e.g., Risaliti & Lusso 2019), but within EAoU is naturally resolved once the datasets are combined, yielding a consistent $\Omega_m \approx 0.23$.

As shown in Figure 5, the Ω_m–α confidence contours provide direct geometric evidence that ΛCDM ($\alpha = 0$) is excluded at $>10\sigma$ significance, while EAoU yields a consistent solution across supernovae, GRBs, and quasars.

5.3. Addressing Potential Concerns

In this section, we discuss potential concerns regarding the EAoU framework and clarify how these issues are addressed, both conceptually and within the data analysis.

Extra parameter : EAoU introduces a single new parameter α. The improvement in χ^2 ($\Delta\chi^2 \approx -1808$) is far larger than the penalty terms in information criteria. Both ΔAIC and ΔBIC decisively favor EAoU, confirming that the inclusion of α is statistically justified

Systematics : The results are consistent across three independent probes—supernovae, GRBs, and quasars—each subject to distinct calibration methods and astrophysical systematics. Calibration uncertainties are absorbed through the standard nuisance parameter μ_0, ensuring robustness against absolute magnitude or H_0 priors. The consistent preference for $\alpha < 0$ across all probes argues strongly against the signal being an artifact of dataset-specific systematics.

Compatibility with Early-universe physics: EAoU modifies late-time distance inferences only, leaving early-universe microphysics untouched. Constraints from big bang nucleosynthesis, recombination, and the CMB power spectrum remain intact. BAO and CMB distance measures can therefore be consistently reinterpreted within the EAoU framework without conflict.

Comoving frame objection: While the comoving observer framework has historically been the standard in cosmology, it is neither physically mandated nor the only viable relativistic approach. EAoU provides an alternative observer-centric formulation that remains fully consistent with general relativity while aligning better with high-redshift observations.

5.4. Connection to Cosmological Tensions

EAoU provides a unifying perspective on several outstanding tensions:

Hubble tension: By reframing H_0 as an effective expansion rate, EAoU alleviates the discrepancy between local distance-ladder determinations and early-universe CMB inferences.

Age tension: The effective age of ~45 Gyr naturally accommodates the existence of old stellar populations and mature galaxies at high redshift, which otherwise challenge ΛCDM.

Distance-ladder anomalies: The reshaped luminosity distance relation directly impacts the redshift regime where supernova, GRB, and quasar discrepancies emerge, offering a coherent explanation.

6. Conclusions

We have introduced and empirically validated the **Effective Age of the Universe (EAoU)** as an observer-centric reformulation of cosmic time, grounded in the relativistic principle of time dilation. Using a combined dataset of **4284 cosmological probes**—Pantheon+SH0ES supernovae, gamma-ray

 doi:10.20944/preprints202509.1394.v1

bursts, and quasars—we demonstrated that EAoU decisively outperforms ΛCDM. The improvement of $\Delta\chi^2 \approx -1808$ is achieved with only one additional parameter, while recovering physically consistent values of $\Omega_m \simeq 0.23$. The best-fit correction parameter ($\alpha \simeq -0.48$) implies an effective cosmic age of ~45 Gyr, in close agreement with our earlier theoretical predictions [1–5].

EAoU represents a **minimal yet physically motivated extension** to the FLRW–ΛCDM framework. By replacing the comoving abstraction with the observer's proper-time perspective, it provides a natural explanation for high-redshift anomalies, reframes the Hubble tension in terms of an effective expansion rate, and resolves the long-standing age problem.

On a cosmic scale, the evidence presented here demonstrates that at high redshift the Hubble diagram is better fit when cumulative time dilation is included, as prescribed by General Relativity. By contrast, the comoving frame abstraction systematically suppresses this effect, leading to poorer fits and unphysical parameter values. With over four thousand probes spanning supernovae, gamma-ray bursts, and quasars, our analysis shows that cumulative relativistic time dilation is not only a theoretical inevitability but also an empirical necessity. This constitutes a direct revalidation of Einstein's General Theory of Relativity at cosmological scales, extending its observational support beyond the classical solar-system and binary-pulsar domains into the largest structures of the universe.

A brief critique of the comoving observer convention is warranted. While historically invaluable for simplifying the FLRW equations, the comoving frame was designed to avoid the complexities of relativistic time dilation in early cosmological modeling. In doing so, however, it abstracts away from the proper-time measure of physical observers. The EAoU framework restores this neglected aspect, demonstrating that incorporating observer-centric time not only honors the relativistic principle but also resolves long-standing cosmological tensions.

Looking forward, future work will:

- extend EAoU to the interpretation of BAO and CMB distance measures,
- test its implications for structure formation and clustering, and

refine the allowed parameter space using next-generation surveys (e.g. LSST, Euclid, JWST).

EAoU thus emerges as both a **theoretical necessity** and an **empirically validated framework shift** in cosmology, offering a unified and observer-centric framework to address multiple cosmological tensions.

7. Software & Data Availability

The analysis was performed using Jupyter and Google Colab notebooks that implement χ^2 fitting routines for both ΛCDM and EAoU models. Supernova distances were drawn from the Pantheon+SH0ES release [6–10], while gamma-ray burst and quasar catalogs were provided as standardized CSV tables containing the columns `(ID, z, μ, σμ, source)`. All datasets were homogenized into `(z, μ, σμ)` arrays and combined into a joint database of 4,284 objects spanning supernovae, GRBs, and quasars.

The χ^2 likelihood function was evaluated with analytic marginalization over the nuisance parameter μ_0, which absorbs the absolute calibration degeneracy with H_0. Analysis outputs, including best-fit parameters, $\Delta\chi^2$ values, and figures, are saved in machine-readable formats (CSV/JSON) and archived alongside this manuscript. The full code repository and input data schema are openly available at (https://github.com/jhossain1962/EAoU-Cosmology/) , enabling full reproducibility of the results.

References

1. Hossain, J. (2025). Effective Age of Universe: A New Concept Resolving Cosmological Tensions. Preprints.org. https://doi.org/10.20944/preprints202508.0758.v1
2. J. Hossain, Estimating the Effective Age of the Universe under Time Dilation: ~45 Gyr. Zenodo (2025). doi:10.5281/zenodo.16741625

3. J. Hossain, Relativistic Reformulation within the FLRW–ΛCDM Framework. Zenodo (2025). doi:10.5281/zenodo.16741568
4. J. Hossain, Effective Age of Universe: A New Concept Resolving Cosmological Tensions. Zenodo (2025). doi:10.5281/zenodo.16629353
5. J. Hossain, Effective Age of the Universe: Application of Relativistic Time Dilation. ResearchGate (2025). doi:10.13140/RG.2.2.25271.43688
6. Brout, D., Scolnic, D., Popovic, B., Riess, A.G., Carr, A., Chen, R., Davis, T.M., Dwomoh, A., Fischer, J.A., Jones, D.O., et al. *The Pantheon+ Analysis: Cosmological Constraints.* Astrophys. J. **938**, 110 (2022). https://doi.org/10.3847/1538-4357/ac8e04
7. Riess, A.G., Yuan, W., Macri, L.M., et al. (2022). *A Comprehensive Measurement of the Local Value of the Hubble Constant with 1 km/s/Mpc Uncertainty from the Hubble Space Telescope and the SH0ES Team*. Astrophys. J. Lett. 934, L7.
8. **Risaliti, G., Lusso, E. (2019).** *Cosmological constraints from the Hubble diagram of quasars*. **Nature Astronomy 3**, 272–277. arXiv:1811.02590.
9. Dainotti, M.G., Petrosian, V., Willingale, R., et al. (2013). *Determination of the intrinsic Luminosity–Time correlation in the X-ray afterglow of GRBs*. Astrophys. J. **774**, 157.
10. Amati, L., et al. (2024). *Detection of gamma-ray burst Amati relation based on Hubble data and Pantheon+*. Eur. Phys. J. C 84, 304.
11. Conley, A., Guy, J., Sullivan, M., Regnault, N., Astier, P., Balland, C., Basa, S., Carlberg, R.G., Fouchez, D., Hardin, D., et al. *Supernova Constraints and Systematic Uncertainties from the First Three Years of the Supernova Legacy Survey.* Astrophys. J. Suppl. Ser. **192**, 1 (2011). https://doi.org/10.1088/0067-0049/192/1/1
12. Adam G. Riess *et al* 2001 *ApJ* **560** 49**DOI** 10.1086/322348
13. Riess, A.G., et al. (2016). "A 2.4% Determination of the Local Value of the Hubble Constant." ApJ 826, 56.
14. Byrd, R.H., Lu, P., Nocedal, J., & Zhu, C. (1995). *A Limited Memory Algorithm for Bound Constrained Optimization*. SIAM Journal on Scientific Computing, 16(5), 1190–1208. https://doi.org/10.1137/0916069